Water Research 113 (2017) 97–110

Contents lists available at ScienceDirect

Water Research

journal homepage: www.elsevier.com/locate/watres

Plant-wide modelling of phosphorus transformations in wastewater treatment systems: Impacts of control and operational strategies

K. Solon [a], X. Flores-Alsina [b], C. Kazadi Mbamba [c], D. Ikumi [d], E.I.P. Volcke [e], C. Vaneeckhaute [f], G. Ekama [d], P.A. Vanrolleghem [g], D.J. Batstone [c], K.V. Gernaey [b], U. Jeppsson [a, *]

[a] Division of Industrial Electrical Engineering and Automation, Department of Biomedical Engineering, Lund University, Box 118, SE-221 00, Lund, Sweden
[b] CAPEC-PROCESS Research Center, Department of Chemical and Biochemical Engineering, Technical University of Denmark, Building 229, DK-2800, Kgs. Lyngby, Denmark
[c] Advanced Water Management Centre, The University of Queensland, St Lucia, Brisbane, Queensland 4072, Australia
[d] Water Research Group, Department of Civil Engineering, University of Cape Town, Rondebosch, 7700, South Africa
[e] Department of Biosystems Engineering, Ghent University, Coupure Links 653, B-9000, Gent, Belgium
[f] BioEngine, Department of Chemical Engineering, Université Laval, Québec, QC, G1V 0A6, Canada
[g] modelEAU, Département de Génie Civil et de Génie des Eaux, Université Laval, Québec, QC, G1V 0A6, Canada

ARTICLE INFO

Article history:
Received 5 October 2016
Received in revised form
2 February 2017
Accepted 3 February 2017
Available online 6 February 2017

Keywords:
Benchmarking
Control strategies
Multiple mineral precipitation
Physico-chemical modelling
Nutrient removal
Struvite recovery

ABSTRACT

The objective of this paper is to report the effects that control/operational strategies may have on plant-wide phosphorus (P) transformations in wastewater treatment plants (WWTP). The development of a new set of biological (activated sludge, anaerobic digestion), physico-chemical (aqueous phase, precipitation, mass transfer) process models and model interfaces (between water and sludge line) were required to describe the required tri-phasic (gas, liquid, solid) compound transformations and the close interlinks between the P and the sulfur (S) and iron (Fe) cycles. A modified version of the Benchmark Simulation Model No. 2 (BSM2) (open loop) is used as test platform upon which three different operational alternatives (A_1, A_2, A_3) are evaluated. Rigorous sensor and actuator models are also included in order to reproduce realistic control actions. Model-based analysis shows that the combination of an ammonium (S_{NH_x}) and total suspended solids (X_{TSS}) control strategy (A_1) better adapts the system to influent dynamics, improves phosphate (S_{PO_4}) accumulation by phosphorus accumulating organisms (X_{PAO}) (41%), increases nitrification/denitrification efficiency (18%) and reduces aeration energy ($E_{aeration}$) (21%). The addition of iron (X_{FeCl_3}) for chemical P removal (A_2) promotes the formation of ferric oxides (X_{HFO-H}, X_{HFO-L}), phosphate adsorption ($X_{HFO-H,P}$, $X_{HFO-L,P}$), co-precipitation ($X_{HFO-H,P,old}$, $X_{HFO-L,P,old}$) and consequently reduces the P levels in the effluent (from 2.8 to 0.9 g P.m^{-3}). This also has an impact on the sludge line, with hydrogen sulfide production (G_{H_2S}) reduced (36%) due to iron sulfide (X_{FeS}) precipitation. As a consequence, there is also a slightly higher energy production ($E_{production}$) from biogas. Lastly, the inclusion of a stripping and crystallization unit (A_3) for P recovery reduces the quantity of P in the anaerobic digester supernatant returning to the water line and allows potential struvite ($X_{MgNH_4PO_4}$) recovery ranging from 69 to 227 kg.day^{-1} depending on: (1) airflow ($Q_{stripping}$); and, (2) magnesium ($Q_{Mg(OH)_2}$) addition. All the proposed alternatives are evaluated from an environmental and economical point of view using appropriate performance indices. Finally, some deficiencies and opportunities of the proposed approach when performing (plant-wide) wastewater treatment modelling/engineering projects are discussed.

* Corresponding author.
E-mail address: ulf.jeppsson@iea.lth.se (U. Jeppsson).

http://dx.doi.org/10.1016/j.watres.2017.02.007
0043-1354/

Nomenclature

A	Alternative
AD	Anaerobic digestion
ADM1	Anaerobic Digestion Model No. 1
AER	Aerobic section
ANAER	Anaerobic section
ANOX	Anoxic section
ASM	Activated Sludge Model
ASM2d	Activated Sludge Model No. 2d
BOD	Biological oxygen demand
BSM2	Benchmark Simulation Model No. 2
CBIM	Continuity-based interfacing method
COD	Chemical oxygen demand
$CONV_{AD\text{-}AS}$	Conversion ADM1 – ASM2d interface
$CONV_{AS\text{-}AM}$	Conversion ASM2d – ADM1 interface
DO	Dissolved oxygen
EQI	Effluent quality index
Fe	Iron
GAO	Glycogen accumulating organisms
G_{CH_4}	Methane production rate (gas) (ADM1) ($kg.day^{-1}$)
G_{CO_2}	Carbon dioxide production rate (gas) (ADM1) ($kg.day^{-1}$)
G_{H2}	Hydrogen production rate (gas) (ADM1) ($kg.day^{-1}$)
G_{H_2S}	Hydrogen sulfide production rate (gas) (ADM1) ($kg.day^{-1}$)
MMP	Multiple mineral precipitation
OCI	Operational cost index
P	Phosphorus
PAO	Phosphorus accumulating organisms
PHA	Polyhydroxyalkanoates
PP	Polyphosphates
PRIM	Primary clarifier
$PROCESS_{AD\text{-}AS}$	Process ADM1– ASM2d interface
$PROCESS_{AS\text{-}AD}$	Process ASM2d – ADM1 interface
Q_{intr}	Internal recycle flow rate (between AER and ANOX) ($m^3.day^{-1}$)
S	Sulfur
SEC2	Secondary clarifier
SI	Saturation index
SRB	Sulfate-reducing bacteria
STRIP	Stripping unit
S_A	Acetate (ASM2d) (g $COD.m^{-3}$)
S_{aa}	Amino acids (ADM1) (kg $COD.m^{-3}$)
S_{ac}	Total acetic acid (ADM1) (kg $COD.m^{-3}$)
S_{an}	Anions (ADM1) ($kmol.m^{-3}$)
S_{bu}	Total butyric acid (ADM1) (kg $COD.m^{-3}$)
S_{Ca}	Calcium (ASM2d, ADM1) ($g.m^{-3}$) ($kmol.m^{-3}$)
S_{cat}	Soluble cations (ADM1) ($kmol.m^{-3}$)
S_{Cl}	Chloride (ASM2d, ADM1) ($g.m^{-3}$) ($kmol.m^{-3}$)
S_F	Fermentable substrate (ASM2d) (g $COD.m^{-3}$)
S_{fa}	Fatty acids (ADM1) (kg $COD.m^{-3}$)
$S_{Fe^{2+}}$	Iron (II) (ASM2d, ADM1) ($g.m^{-3}$) ($kmol.m^{-3}$)
$S_{Fe^{3+}}$	Iron (III) (ASM2d, ADM1) ($g.m^{-3}$) ($kmol.m^{-3}$)
S_{H_2}	Hydrogen (ADM1) (kg $COD.m^{-3}$)
S_{IC}	Inorganic carbon (ADM1) ($kmol.m^{-3}$)
S_{IN}	Inorganic nitrogen (ADM1) ($kmol.m^{-3}$)
S_{IP}	Inorganic phosphorus (ADM1) ($kmol.m^{-3}$)
S_{IS}	Inorganic total sulfides (ADM1) (kg $COD.m^{-3}$)
S_K	Potassium (ASM2d, ADM1) ($g.m^{-3}$) ($kmol.m^{-3}$)
S_{Mg}	Magnesium (ASM2d, ADM1) ($g.m^{-3}$) ($kmol.m^{-3}$)
S_{Na}	Sodium (ASM2d, ADM1) ($g.m^{-3}$) ($kmol.m^{-3}$)
S_{NH_x}	Ammonium plus ammonia nitrogen (ASM2d) ($g.m^{-3}$)
S_{NO_x}	Nitrate plus nitrite (ASM2d) ($g.m^{-3}$)
S_{pro}	Total propionic acid (ADM1) (kg $COD.m^{-3}$)
S_{PO_4}	Phosphate (ASM2d) ($g.m^{-3}$)
S_{su}	Sugars (ADM1) (kg $COD.m^{-3}$)
S_{S_0}	Elemental sulfur (ADM1) ($kmol.m^{-3}$)
S_{SO_4}	Sulfate (ASM2d, ADM1) ($g.m^{-3}$) ($kmol.m^{-3}$)
S_{va}	Total valeric acid (ADM1) (kg $COD.m^{-3}$)
THK/FLOT	Thickener/flotation
TIV	Time in violation
TKN	Total Kjeldahl nitrogen
TN	Total nitrogen
TP	Total phosphorus
TSS	Total suspended solids
VFA	Volatile fatty acids
WRRF	Water resource recovery facility
WWTP	Wastewater treatment plant
X_A	Autotrophic biomass (ASM2d) (g $COD.m^{-3}$)
X_{ac}	Acetate degraders (ADM1) (kg $COD.m^{-3}$)
X_{AlPO_4}	Aluminum phosphate (ASM2d, ADM1) ($g.m^{-3}$) ($kmol.m^{-3}$)
X_B	Total biomass (ADM1) (kg $COD.m^{-3}$)
X_c	Composite material (ADM1) (kg $COD.m^{-3}$)
X_{C4}	Butyrate and valerate degraders (ADM1) (kg $COD.m^{-3}$)
X_{CaCO_3}	Calcite (ASM2d, ADM1) ($g.m^{-3}$) ($kmol.m^{-3}$)
$X_{CaCO_{3a}}$	Aragonite (ASM2d, ADM1) ($g.m^{-3}$) ($kmol.m^{-3}$)
$X_{Ca_3(PO_4)_2}$	Amorphous calcium phosphate (ASM2d, ADM1) ($g.m^{-3}$) ($kmol.m^{-3}$)
$X_{Ca_5(PO_4)_3(OH)}$	Hydroxylapatite (ASM2d, ADM1) ($g.m^{-3}$) ($kmol.m^{-3}$)
$X_{Ca_8H_2(PO_4)_6}$	Octacalcium phosphate (ASM2d, ADM1) ($g.m^{-3}$) ($kmol.m^{-3}$)
X_{ch}	Carbohydrates (ADM1) (kg $COD.m^{-3}$)
X_{FeS}	Iron sulfide (ASM2d, ADM1) ($mol.L^{-1}$) ($kmol.m^{-3}$)
X_H	Heterotrophic biomass (ASM2d) (g $COD.m^{-3}$)
X_{HFO-H}	Hydrous ferric oxide with high number of active sites (ASM2d, ADM1) ($g.m^{-3}$) ($kmol.m^{-3}$)
$X_{HFO-H,P}$	X_{HFO-H} with bounded adsorption sites (ASM2d, ADM1) ($g.m^{-3}$) ($kmol.m^{-3}$)
$X_{HFO-H,P,old}$	Old $X_{HFO-H,P}$ with bounded adsorption sites (ASM2d, ADM1) ($g.m^{-3}$) ($kmol.m^{-3}$)
X_{HFO-L}	Hydrous ferric oxide with low number of active sites (ASM2d, ADM1) ($g.m^{-3}$) ($kmol.m^{-3}$)
$X_{HFO-L,P}$	X_{HFO-L} with bounded adsorption sites (ASM2d, ADM1) ($g.m^{-3}$) ($kmol.m^{-3}$)
$X_{HFO-L,P,old}$	Old $X_{HFO-L,P}$ with bounded adsorption sites (ASM2d, ADM1) ($g.m^{-3}$) ($kmol.m^{-3}$)
$X_{HFO-old}$	Inactive X_{HFO} (ASM2d, ADM1) ($g.m^{-3}$) ($kmol.m^{-3}$)
X_i	Inert particulate organics (ASM2d, ADM1) (g $COD.m^{-3}$) (kg $COD.m^{-3}$)
$X_{KNH_4PO_4}$	K-struvite (ASM2d, ADM1) ($g.m^{-3}$) ($kmol.m^{-3}$)
X_{li}	Lipids (ADM1) (kg $COD.m^{-3}$) ($g.m^{-3}$) ($kmol.m^{-3}$)
X_{MgCO_3}	Magnesite (ASM2d, ADM1) ($g.m^{-3}$) ($kmol.m^{-3}$)
X_{MgHPO_4}	Newberyite (ASM2d, ADM1) ($g.m^{-3}$) ($kmol.m^{-3}$)
$X_{MgNH_4PO_4}$	Struvite (ASM2d, ADM1) ($g.m^{-3}$) ($kmol.m^{-3}$)
X_{PAO}	Phosphorus accumulating organisms (ASM2d, ADM1) (g $COD.m^{-3}$) (kg $COD.m^{-3}$)
X_{PHA}	Polyhydroxyalkanoates (ASM2d, ADM1) (g $COD.m^{-3}$) (kg $COD.m^{-3}$)
X_{PP}	Polyphosphates (ASM2, ADM1) ($g.m^{-3}$) ($kmol.m^{-3}$)
X_{pr}	Proteins (ADM1) (kg $COD.m^{-3}$)
X_{pro}	Propionate degraders (ADM1) (kg $COD.m^{-3}$)
X_{SRB}	Sulfate-reducing bacteria (ADM1) (kg $COD.m^{-3}$)
Z_i	Chemical species concentration of species i (algebraic variable of the physico-chemistry module) ($kmol.m^{-3}$)

1. Introduction

The importance of plant-wide modelling has been emphasized by the chemical engineering community for a long time and the wastewater industry is also realizing the benefits of this approach (Skogestad, 2000; Gernaey et al., 2014). A wastewater treatment plant should be considered as an integrated process, where primary/secondary clarifiers, activated sludge reactors, anaerobic digesters, thickener/flotation units, dewatering systems, storage tanks, etc. are linked together and need to be operated and controlled not as individual unit operations, but taking into account all the interactions amongst the processes (Jeppsson et al., 2013). For this reason, during the last years wastewater engineering has promoted the development of integrated modelling tools handling these issues (Barker and Dold, 1997; Grau et al., 2007; Ekama, 2009; Nopens et al., 2010; Gernaey et al., 2014). Plant-wide models substantially increase the number of potential operational strategies that can be simulated, and thereby enable the study of a new dimension of control possibilities, such as studying the impact of activated sludge control strategies on the sludge line (Jeppsson et al., 2007), the effect of primary sedimentation on biogas production (Flores-Alsina et al., 2014a) and the handling of nitrogen-rich anaerobic digester supernatant (Volcke et al., 2006a; Ruano et al., 2011; Flores-Alsina et al., 2014a).

Although being valuable tools, the state of the art is that these plant-wide models are limited to the prediction of plant-wide organic carbon and nitrogen, and they are not properly taking into account the transformation of phosphorus (P) and its close interlinks with the sulfur (S) and iron cycles (Fe), particularly in a plant-wide context (Batstone et al., 2015). Phosphorus modelling is an essential requirement, particularly considering its role in eutrophication of many catchments and its potential re-use as a fertilizer (Verstraete et al., 2009). Therefore, this is an important issue for future model application and it will become of paramount importance during the transition of wastewater treatment plants (WWTP) to water resource recovery facilities (WRRFs), which will change the requirements for model-based analysis significantly for wastewater engineering studies (Vanrolleghem et al., 2014; Vanrolleghem and Vaneeckhaute, 2014).

The Activated Sludge Model No. 2d (ASM2d) specifically considers the role of phosphorus accumulating organisms (PAO) in the water line (Henze et al., 2000). Similar P-related processes should be included in the Anaerobic Digestion Model No. 1 (ADM1) (Batstone et al., 2002) as stated by Ikumi and co-workers (Ikumi et al., 2011, 2014). Potential uptake of organics by PAO to form polyhydroxyalkanoates (PHA) with the subsequent release of polyphosphates (PP) can also have an important effect on the anaerobic digestion (AD) products (biogas, precipitates) (Wang et al., 2016; Flores-Alsina et al., 2016). Nevertheless the ASM family (specifically the ASM2d for phosphorus) (Henze et al., 2000) and ADM1 (Batstone et al., 2002) are inadequate to describe plant-wide P transformations. Part of this is because the physico-chemical formulations in those models do not consider more complex phenomena in which P is involved. Indeed, P trivalence gives a strong non-ideal behaviour, which requires amongst other factors, continuous ionic strength tracking, extensive consideration of activities instead of molar concentrations and inclusion of complexation/ion pairing processes (Musvoto et al., 2000; Serralta et al., 2004; Solon et al., 2015; Flores-Alsina et al., 2015; Lizarralde et al., 2015). The latter is crucial to correctly describe chemical precipitation and predict the fate of phosphorus compounds, and to properly predict nutrient cycling through the entire plant (van Rensburg et al., 2003; Barat et al., 2011; Hauduc et al., 2015; Kazadi Mbamba et al., 2015a,b). There is also a general lack of consideration of biological and chemical transformation of Fe and S, throughout both aerobic and anaerobic stages. Specifically, the sulfur cycle regulates Fe availability (and Fe changes valency through oxidation/reduction) which then controls iron-phosphate complexing (Gutierrez *et al.*, 2010; Flores-Alsina et al., 2016). While biological and chemical complexation reactions of P have been described in the AD unit, these have not generally been considered in plant-wide interactions with the Fe/S cycles.

Model interfacing is also an important aspect to consider (Batstone et al., 2015) unless integrated plant-wide models with a single set of state variables are used (Barker and Dold, 1997; Grau et al., 2007; Ekama et al., 2006; Barat et al., 2013). Plant-wide modelling requires elemental mass balance verification (Hauduc et al., 2010) and continuity checking for all the components included in the model (Volcke et al., 2006b; Zaher et al., 2007; Nopens et al., 2009). Therefore, the quantities of C, N, P, Fe and S should be the same before and after an interface (Flores-Alsina et al., 2016). The main advantage of using an interface-based approach with respect to other integrated methodologies is that the original model structure can be used, and there is thus no need for state variable representation in all process units with the resulting increased use of computational power, model complexity and adverse model stability characteristics (Grau et al., 2009).

The main objective of this paper is to present (for the first time): (1) an approach for mechanistic description of all the main biological and physico-chemical processes required to predict organic P fluxes simultaneously in both water and sludge lines in the WWTP under different operational modes; (2) an analysis of the interactions between P, S and Fe on a plant-wide level; (3) a quantification of the compound fluxes and pH variations in each unit and through the entire plant; and, (4) an evaluation of the different operational/control strategies aimed at maximizing energy production, resource recovery and reduction of the environmental impact and operating expenses measured as effluent quality (*EQI*) and operational cost indices (*OCI*) (Copp, 2002; Nopens et al., 2010). The paper details the development of the new plant-wide model by presenting sequentially the different included sub-elements as well as the integration/interfacing aspects. The capabilities/potential of the proposed approach is illustrated with several case studies. Lastly, opportunities and limitations that arise from utilization of the new model are discussed as well.

2. Model description

2.1. Biological models

Sections 2.1.1 and 2.1.2 describe the additional processes and state variables included in the ADM1 and ASM2d, respectively, in order to take into account biologically mediated phosphorus transformations correctly. Additional modifications, with special emphasis to link the ADM and ASM with a physico-chemical model, are described in Section 3 (Model integration). Model details, mass balances and continuity verification can be found in the spreadsheet files provided within the Supplemental Information Section.

2.1.1. Anaerobic digestion model (ADM)

The ADM1 version, implemented in the plant-wide context provided by the Benchmark Simulation Model No. 2 (BSM2) (Batstone et al., 2002; Rosen et al., 2006) is extended with P, S and Fe interactions (Flores-Alsina et al., 2016). Phosphorus transformations account for kinetic decay of polyphosphates (X_{PP}) and potential uptake of volatile fatty acids (VFA) to produce polyhydroxyalkanoates (X_{PHA}) by phosphorus accumulating organisms (X_{PAO}) (Henze et al., 2000; Harding et al., 2011; Ikumi et al., 2011; Wang et al., 2016). Biological production of sulfides (S_{IS}) is

described by means of sulfate-reducing bacteria (X_{SRB}) utilising hydrogen (autolithotrophically) as electron source (Batstone, 2006). Potential hydrogen sulfide (Z_{H_2S}) inhibition and stripping to the gas phase (G_{H_2S}) are considered (Fedorovich et al., 2003; Pokorna-Krayzelova et al., 2017). Finally, chemical iron (III) ($S_{Fe^{3+}}$) reduction to iron (II) ($S_{Fe^{2+}}$) is accounted for by using hydrogen (S_{H_2}) and sulfides (S_{IS}) as electron donors (Stumm and Morgan, 1996).

2.1.2. Activated sludge model (ASM)

A modified version of the Activated Sludge Model No. 2d (ASM2d) is selected to describe organic carbon, nitrogen and phosphorus transformations in the biological reactor (Henze et al., 2000). In this implementation, biomass decay rates are electron-acceptor dependent (Siegrist et al., 1999; Gernaey and Jørgensen, 2004). Potassium (S_K) and magnesium (S_{Mg}) are accounted for as new state variables and are included in the stoichiometry of formation and release of polyphosphates (X_{PP}). Another modification with respect to the original ASM2d is that total suspended solids is calculated from its constituents ($X_{TSS} = X_{VSS} + X_{ISS}$ are described separately) (Ekama and Wentzel, 2004; Ekama et al., 2006) compared to the previous implementations wherein TSS is calculated as the sum of the assumed TSS content of each of the particulate state variables. This is mainly because the constituents of the inorganic suspended solids (X_{ISS}) are explicitly calculated as state variables with a contribution from polyphosphate (X_{PP}) in the activated sludge system. The model is also upgraded to describe the fate (oxidation/reduction reactions) of sulfur ($S_{SO_4^{2-}}$, S_{S_0}, S_{IS}) and iron ($S_{Fe^{3+}}$, $S_{Fe^{2+}}$) compounds in anaerobic, anoxic and aerobic conditions. Sulfate reduction is assumed to be biologically mediated by means of SRB (X_{SRB}) using two potential electron donors (S_A, S_F). Sulfide (S_{IS}) and ($S_{Fe^{2+}}$) oxidation is described as a purely chemical reaction using different electron acceptors (S_{O_2}, S_{NO_x}) (Batstone, 2006; Batstone et al., 2015; Gutierrez et al., 2010; Stumm and Morgan, 1996).

2.2. Physico-chemical models (PCM)

2.2.1. pH and ion speciation/pairing

In this study a general aqueous phase chemistry model describing pH variation and ion speciation/pairing in both ASM and ADM is used (Solon et al., 2015; Flores-Alsina et al., 2015). The model corrects for ionic strength via the Davies' approach to consider chemical activities instead of molar concentrations, performing all the calculations under non-ideal conditions. The general acid-base equilibria are formulated as a set of implicit algebraic equations (IAEs) and solved separately at each time step of the ordinary differential equation (ODE) solver using an extended multi-dimensional Newton-Raphson algorithm (Solon et al., 2015; Flores-Alsina et al., 2015). Acid-base parameters and activity coefficients are corrected for temperature effects. The species concentrations are expressed by a common nomenclature (Z_i) (Solon et al., 2015) and participate in physico-chemical processes such as gas exchange and mineral precipitation (see Sections 2.2.2 and 2.2.3).

2.2.2. Multiple mineral precipitation (MMP)

In this model, precipitation equations are described as a reversible process using the saturation index (*SI*) as the chemical driving force. The *SI* represents the logarithm of the ratio between the product of the respective activities of reactants that are each raised to the power of their respective stoichiometric coefficient, and the solubility product constant (K_{sp}) (temperature corrected). If $SI < 0$ the liquid phase is assumed to be undersaturated and a mineral might dissolve into the liquid phase, while if $SI > 0$ the liquid phase is assumed to be supersaturated and mineral precipitation might occur (Stumm and Morgan, 1996). The precipitation reaction rate depends on the kinetic rate coefficient, the concentration of the different species (Z_i), mineral solid phase (X_i) and the order of the reaction (n) (Kazadi Mbamba et al., 2015a,b). The proposed MMP model includes the minerals: calcite (X_{CaCO_3}), aragonite ($X_{CaCO_{3a}}$), amorphous calcium phosphate ($X_{Ca_3(PO_4)_2}$), hydroxylapatite ($X_{Ca_5(PO_4)_3(OH)}$), octacalcium phosphate ($X_{Ca_8H_2(PO_4)_6}$), struvite ($X_{MgNH_4PO_4}$), newberyite (X_{MgHPO_4}), magnesite (X_{MgCO_3}), k-struvite ($X_{KNH_4PO_4}$) and iron sulfide (X_{FeS}). A special formulation is necessary to correctly describe precipitation of hydrous ferric oxides (X_{HFO-H}, X_{HFO-L}), phosphate adsorption ($X_{HFO-H,P}$, $X_{HFO-L,P}$) and co-precipitation ($X_{HFO-H,P,old}$, $X_{HFO-L,P,old}$) (Hauduc et al., 2015), since this is an adsorption rather than a precipitation reaction. Kinetic parameters were taken from Kazadi Mbamba et al. (2015a,b) and Hauduc et al. (2015).

2.2.3. Gas-liquid transfer

In open reactors, gas-liquid transfer is described as a function of the difference between the saturation concentration and the actual concentration of the gas dissolved in the liquid and the contact area between the gaseous and the aqueous phase (Truskey et al., 2009). The saturation concentration of the gas in the liquid is given by Henry's law of dissolution, which states that the saturation concentration is equal to the product of Henry's constant (K_H) multiplied by the partial pressure of the gas (P_i). The mass transfer rate constant ($K_L a_i$) is calculated for each gaseous component ($i = Z_{CO_2}$, Z_{H_2S}, Z_{NH_3} and S_{N_2}). This $K_L a_i$ is calculated with a proportionality factor relative to the reference compound oxygen ($K_L a_{O2}$). The proportionality factor depends on the relation between the diffusivity of the gas in the liquid (D_i) over the diffusivity of oxygen in the liquid (D_{O_2}) (Musvoto et al., 2000). This does not apply for $K_L a_{NH3}$ since NH_3 is a highly soluble gas and thus its mass transfer is controlled by the transfer rate in the gas phase (Lizarralde et al., 2015). In closed reactors, mass transfer between the liquid and the gas volume is described for selected gases ($i = Z_{CO_2}$, Z_{H_2S}, Z_{NH_3}, S_{CH_4} and S_{H_2}) as described in Rosen et al. (2006).

2.3. Model integration

2.3.1. ASM-PCM interface

The default implementation of the ASM was adjusted in order to include the PCM (additional details can be found in Flores-Alsina et al. (2015)). The main modifications are: (1) the use of inorganic carbon (S_{IC}) instead of alkalinity (S_{ALK}) as a state variable; (2) the inclusion of mass transfer equations for Z_{CO_2}, Z_{H_2S}, Z_{NH_3} and S_{N_2} (Batstone et al., 2015; Lizarralde et al., 2015); (3) additional (and explicit) consideration of multiple cations (S_{cat}: S_K, S_{Na}, S_{Ca}, S_{Mg}) and anions (S_{an}: S_{Cl}) which are tracked as soluble/reactive states; and, (4) chemical precipitation using metal hydroxides (X_{MeOH}) and metal phosphates (X_{MeP}) are omitted since the generalised kinetic precipitation model as described in Kazadi Mbamba et al. (2015a,b) and Hauduc et al. (2015) is used instead. Communication between the different models is straightforward. The outputs of the ASM at each integration step are used as inputs for the aqueous-phase module to estimate pH and ion speciation/pairing (works as a sub-routine) (see Section 2.2.1). The precipitation/stripping equations are formulated as ODEs and included in the overall mass balance.

2.3.2. ADM-PCM interface

The ADM is slightly modified to account for the updated physico-chemical model and new processes. The original pH solver proposed by Rosen et al. (2006) is substituted by the approach presented in Solon et al. (2015) and Flores-Alsina et al. (2015). C, N,

P, O and H fractions are taken from de Gracia et al. (2006). Finally, the original ADM1 pools of undefined cations (S_{cat}) and anions (S_{an}) are substituted for specific compounds (see Section 2.3.1). The existing gas-liquid transfer equations are extended to include Z_{H_2S} and Z_{NH_3} (Rosen et al., 2006). Similarly as for the ASM-PCM interface, the pH and ion speciation/pairing model works as a subroutine, while the multiple precipitation/stripping models are included within the system of ODEs in the ADM.

2.3.3. ASM-ADM-ASM interface

The interfaces between ASM-ADM-ASM are based on the continuity-based interfacing method (CBIM) described in Volcke et al. (2006b), Zaher et al. (2007) and Nopens et al. (2009) to ensure elemental mass and charge conservation. The ASM-ADM-ASM interfaces consider: (1) (instantaneous) processes ($PROCESS_{AS\text{-}AD}$/$PROCESS_{AD\text{-}AS}$); and, (2) (state variable) conversions ($CONV_{AS\text{-}AD}$/$CONV_{AD\text{-}AS}$). On the one hand, the ASM-ADM interface instantaneous processes ($PROCESS_{AS\text{-}AD}$) involve (amongst others) instantaneous removal of COD demanding compounds (i.e. S_{O_2} and S_{NO_3}) and immediate decay of (heterotrophic/autotrophic) biomass. Conversions ($CONV_{AS\text{-}AD}$) require the transformation of soluble fermentable organics (S_F), acetate (S_A) and biodegradable particulate organics (X_S) into amino acids (S_{aa})/sugars (S_{su})/fatty acids (S_{fa}) (soluble) and proteins (X_{pr})/lipids (X_{li})/carbohydrates (X_{ch}) (particulate), respectively. On the other hand, the ADM-ASM interface assumes ($PROCESS_{AD\text{-}AS}$) that all compounds that can be transferred into the gas phase (i.e. S_{H_2} and S_{CH_4}) are stripped, and also immediate decay of the AD biomass takes place. $CONV_{AD\text{-}AS}$ turns all the biodegradable organic particulates (X_{pr}, X_{li}, X_{ch}), organic solubles (S_{aa}, S_{fa}, S_{su}) and volatile fatty acids (S_{ac}, S_{pro}, S_{bu}, S_{va}) into X_S, S_F and S_A, respectively. There is no variation of Fe and S before and after the interface. A comprehensive description with detailed explanation of the involved processes, conversions and mass balance verification can be found in Flores-Alsina et al. (2016).

2.4. Additional elements

2.4.1. Influent generation/modelling principles

The model blocks for: (1) flow rate generation (FLOW); (2) chemical oxygen demand (COD), N and P generation (POLLUTANTS); (3) temperature profile generation (TEMPERATURE); and, (4) sewer network and first flush effect (TRANSPORT) defined in Gernaey et al. (2011) are used to generate the WWTP influent dynamics (12 months period of output data for the evaluation period with a 15 min sampling interval). The resulting daily average influent mass flow rates are 8386 kg COD.d^{-1}, 1014 kg N.d^{-1} and 197 kg P.d^{-1} for COD, N and P, respectively (see Fig. SS1 in Supplemental Information for the influent concentrations). The S:COD ratio is 0.003 kg S.kg COD^{-1} (note that the S influent load is set to a high value to have a noticeable effect in the AD). In addition, cation and anion profiles had to be added. The resulting pH is close to neutrality (pH ~ 7). More information about the flow rate pollution dynamics and how they are handled by the influent generator can be found in Flores-Alsina et al. (2014b), Martin and Vanrolleghem (2014) and Snip et al. (2016).

2.4.2. Ancillary processes and sensor/actuator models

Primary clarification is described according to Otterpohl and Freund (1992). The model is adjusted to reflect the experiments carried out by Wentzel et al. (2006) where biodegradable/unbiodegradable compounds show different settling velocities. The double exponential velocity function proposed by Takács et al. (1991) using a 10-layer reactive configuration (Flores-Alsina et al., 2012) is used as a fair representation of the secondary settling process and reactions occurring in the settler. Several correlations between sludge settleability parameters (such as stirred specific volume index, SSVI, and diluted sludge volume index, DSVI) and the Takács settling parameters (maximum Vesilind settling velocity, v_0, and hindered zone settling parameter, r_h) (Gernaey et al., 2014) have been used (Ekama et al., 1997). A reduction factor in the process kinetics is applied to the reactive secondary settler to obtain more realistic results (Guerrero et al., 2013). Flotation and dewatering units are described in Jeppsson et al. (2007). Biological reactions in both units are included using the simplified approach described in Gernaey et al. (2006). Stripping and crystallization units are described in Kazadi Mbamba et al. (2016). Response time, delay and white noise are included in sensor/actuator models in order to avoid creating unrealistic control applications (Rieger et al., 2003).

2.4.3. Plant layout

The presented set of models is implemented in a plant layout that consists of a primary clarifier (PRIM), an activated sludge unit (AS), a secondary settler (SEC2), a sludge thickener (THK/FLOT), an anaerobic digester (AD), a storage tank (ST) and a dewatering unit (DW). The main modification with respect to the original design (Nopens et al., 2010) relies on the activated sludge (AS) configuration. An anaerobic section (ANAER1, ANAER2) without oxygen (S_{O_2}) and nitrate (S_{NO_x}) is needed to promote anaerobic phosphorus release and to provide the phosphorus accumulating organisms (X_{PAO}) with a competitive advantage over other bacteria. Phosphorus release from the breakdown of polyphosphates (X_{PP}) provides the energy required for anaerobic uptake of polyhydroxyalkanoates (X_{PHA}). Next, PAO grow using intracellular storage products (i.e. X_{PHA}) as a substrate while taking up N and P as nutrients in the anoxic (ANOX1, ANOX2) and aerobic (AER1, AER2, AER3) reactors with oxygen (S_{O_2}) or nitrate (S_{NO_3}) (with less efficiency) as electron acceptors, respectively (see schematics in Fig. 1). It is important to highlight that this configuration does not represent an optimal design to remove P, because the biological P removal is dependent on the N removal via the nitrate concentration recycled to the anaerobic reactor via the underflow recycle (i.e. nitrates overflow may cause the anaerobic reactors to become anoxic). Nevertheless, it exemplifies the retrofit of many (C, N removal) plants adapting their plant layout to satisfy new and stricter effluent requirements (the authors do not presume that the given plant layout is the best configuration for retrofit situations; a Modified UCT or a Johannesburg configuration may be more appropriate). Additional details about the WWTP plant design and default operational conditions can be found in Gernaey et al. (2014) and in the software implementation (see Section 6).

2.4.4. Evaluation criteria

To assess the performance of combined N and P control strategies, an updated set of evaluation criteria are necessary (Jeppsson et al., 2013). The effluent quality index (*EQI*) (a weighted sum of effluent TSS, COD, BOD, TKN and nitrate) is updated to include the additional P load (organic and inorganic). Additional P upgrades have been necessary to include effluent violations (frequency and magnitude) and percentiles. The cost of additional recycles (anoxic, anaerobic), aerators (CO_2 stripping) and chemicals (in case the user wants to evaluate chemical P precipitation and recovery) are also added within the operational cost index (*OCI*). A detailed description of the additional evaluation criteria is given in the Supplemental Information Section.

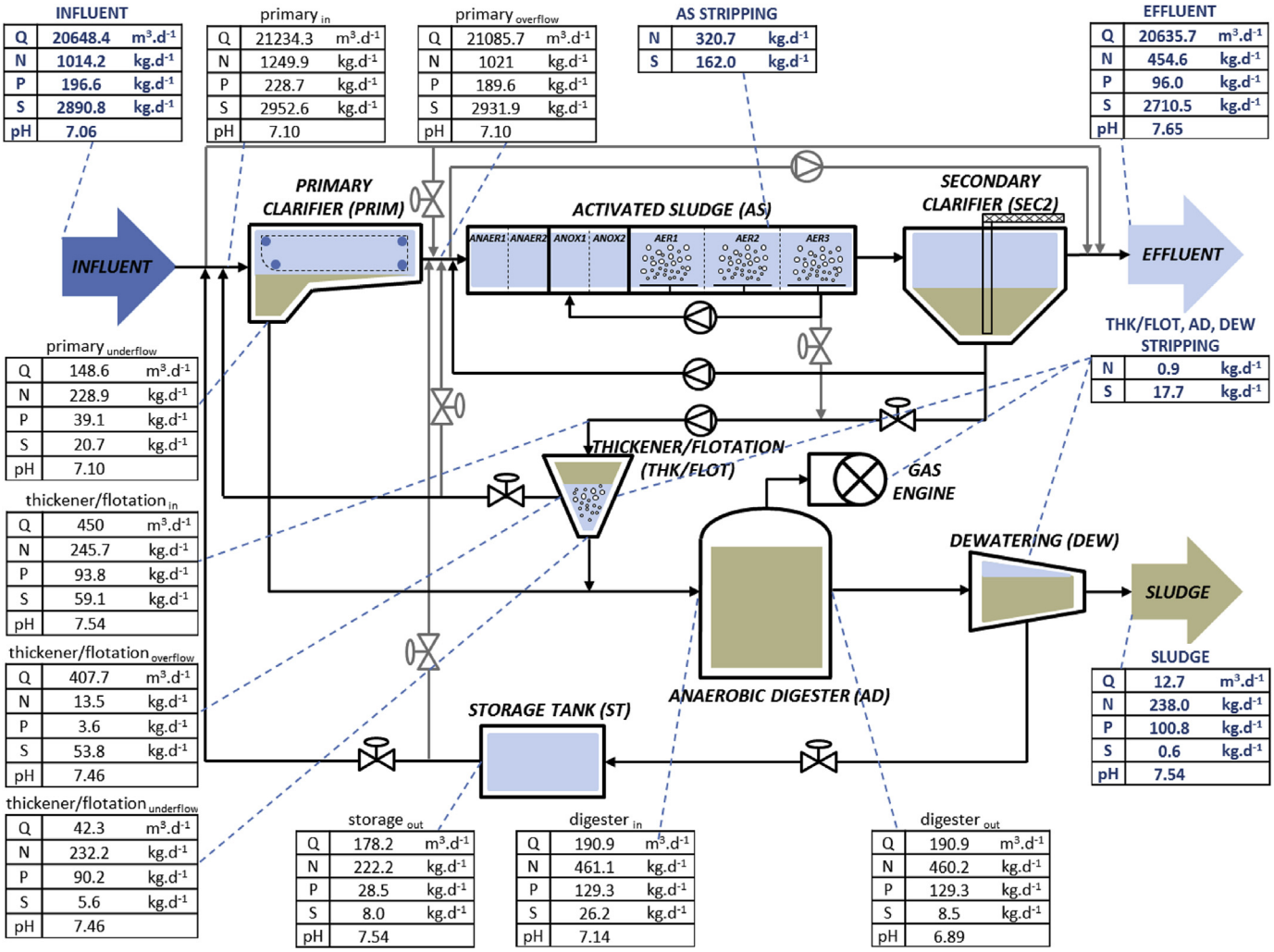

Fig. 1. Block flow diagram including overall and individual (N, P, S, pH) balances for the WWTP under study (scenario A_0).

3. Results and discussion

3.1. Steady-state simulations

The steady-state simulations for the open loop configuration are summarized in Fig. 1 in terms of the plant-wide overall mass balances and the individual ones for C, P, N, S, as well as for pH (plant-wide input and output mass flows in bold). Around 49% of the total incoming P load leaves the plant through the water line (mainly as soluble phosphate, S_{PO_4}). The remaining P (51%) goes to the sludge line (particulate). In the AD unit, soluble S_{PO_4} is substantially increased as a result of biomass (X_B, X_A, X_{PAO}) and polyphosphates (X_{PP}) decay. A fraction (78%) of the incoming P to the digester precipitates ($X_{Ca_3(PO_4)_2}$, $X_{MgNH_4PO_4}$) or becomes part of the organics (X_I, X_S). This will be disposed with the sludge. The remaining P is returned to the water line as soluble phosphate (S_{PO_4}) (22%). This increases the influent P load by almost 20% (see Fig. 1). As a consequence of this extra load the overall plant performance (in terms of phosphorus removal) for the open loop scenario is not good, giving effluent quality values (TP = 4.6 g P.m^{-3}) well above the standards (assumed TP_{limit} = 2.0 g P.m^{-3}).

Most of the nitrogen is depleted before reaching the sludge line (23% remaining) through nitrification-denitrification, assimilation with the biomass and gas stripping. More specifically, around 32% of the incoming N is converted to nitrogen gas (S_{N_2}) and 45% leaves the plant in form of S_{NH_x} or S_{NO_x}. Simulated (N) effluent values (TKN = 2.97 g N.m^{-3} and TN = 9.13 g N.m^{-3}) are well below the limits fixed by the BSM evaluation limit (TKN_{limit} = 4 g N.m^{-3} and TN_{limit} = 15 g N.m^{-3}). The N load going to the sludge line (23%) is basically associated with particulate organics (X_I, X_S) and biomass (X_B, X_A, X_{PAO}). Around 14 and 222 kg N.day^{-1} are returned to the water line after flotation/thickening and dewatering, respectively, adding 23% to the influent N load.

Sulfur arrives to the WWTP under study as sulfate (S_{SO_4}) and sulfides (S_{IS}) (S in the influent is set to a high value for demonstration purposes). In the anaerobic section of the activated sludge process there is a small reduction of S_{SO_4} to S_{IS} by SRB. In the anoxic/aerobic section most of the reduced S is re-oxidized to S_{SO_4} that becomes part of the effluent (93%), a part is stripped to the atmosphere (5%) and a small fraction of S_{SO_4} (2%) is transported to the AD unit where it is converted to hydrogen sulfide gas (G_{H_2S}) (65%) and dissolved sulfides (S_{IS}) (25%) with a concentration of 32 g S.m^{-3} (biogas composition by volume: G_{CH_4} = 62.00 %, G_{CO_2} = 37.46 %, G_{H_2S} = 0.54 %). A small fraction of sulfate remains unconverted (S_{SO_4}) (10%). The soluble S fractions are returned to the water line and are re-oxidized to sulfate in the activated sludge reactor. Compared to the N and P streams, the resulting increase in the influent S load is not very high (increase of 2%).

Table 1
Main characteristics of the implemented control/operational strategies.

Characteristics	DO controller	Ammonium controller	TSS controller	Phosphate controller	Airflow in STRIP	Magnesium controller
Measured variable(s)	S_{O_2} in AER2	S_{NH_x} in AER2	TSS in AER3	S_{PO_4} in AER3	-	-
Controlled Variable(s)	S_{O_2} in AER2	S_{O_2} in AER1, 2 & 3	TSS in AER3	S_{PO_4} in AER3	S_{CO_2} in STRIP	$X_{Mg(OH)_2}$ in STRIP
Set point/critical value	–	2 g N·m^{-3}	4000 g TSS·m^{-3} (if T < 15 °C) 3000 g TSS·m^{-3} (if T > 15 °C)	1 g P·m^{-3}	–	–
Manipulated variable	Q_{air} n AER1, 2 & 3	S_{O_2} set point in AER2	Q_w	Q_{FeCl_3}	$Q_{stripping}$	$Q_{Mg(OH)_2}$
Control algorithm	PI	Cascade PI	Cascade PI	PI	–	–
Applied in control strategies A_i	A_1, A_2 & A_3	A_1, A_2 & A_3	A_1, A_2 & A_3	A_2	A_3	A_3

Influent pH is close to neutrality (pH = 7.06). In this particular case, at the end of the water line pH is increased mainly due to carbon dioxide (Z_{CO_2}) stripping. Nevertheless, in other cases for systems with low buffer capacity, the loss of alkalinity via nitrification might decrease the pH far more strongly (Henze et al., 2008). The almost anaerobic conditions in the first units of the sludge line (secondary settler and thickener/flotation units) promote: (1) fermentation of organic soluble substrate (S_F) to acetate (S_A); and, (2) decay of X_{PP} and subsequent release of S_{IP}. As a consequence, there is a decrease of pH. In the AD, pH is slightly reduced again as a result of multiple mineral precipitation. In the dewatering unit, pH is raised again due to Z_{CO_2} stripping. There is no effect on the influent entering the primary clarifier. Similar observations about pH behaviour through the different plant units are reported in Lizarralde et al. (2015) and Kazadi Mbamba et al. (2016).

3.2. Dynamic simulations

All dynamic simulations (609 days) are preceded by steady-state simulations (300 days) but only the data generated during the final 364 days are used for plant performance evaluation. Default (open loop) operational conditions (Gernaey and Jørgensen, 2004) represent the baseline configuration (A_0) upon which the different operational/control/recovery strategies will be implemented, simulated and evaluated (see Table 1). Fig. 2 shows dynamic profiles for selected influent (Fig. 2a, b), effluent (Fig. 2d, e) and operational (Fig. 2c, f, g, h) variables.

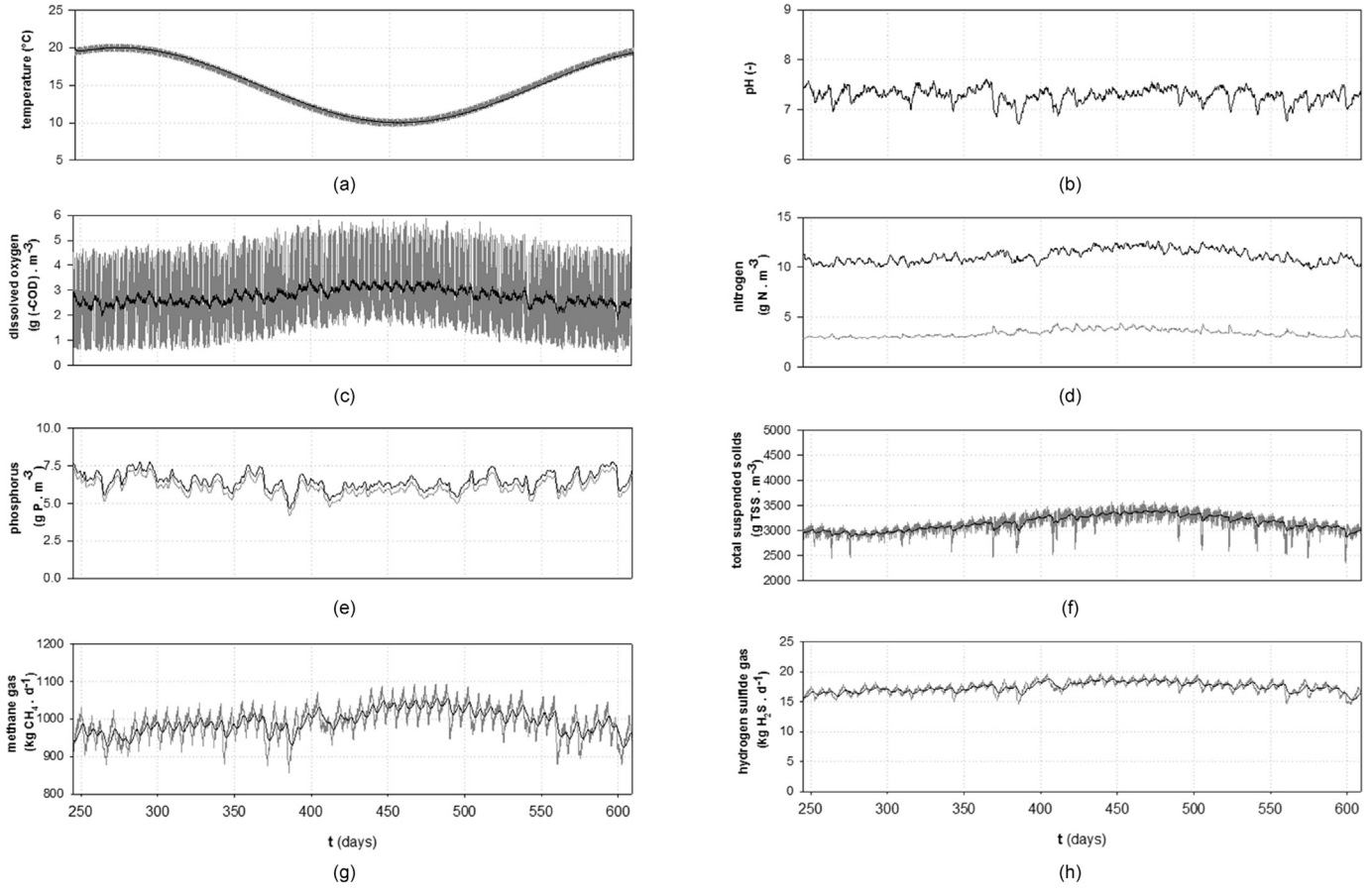

Fig. 2. Dynamic profiles (A_0 = open loop) for: (a) influent temperature; (b) influent pH; (c) dissolved oxygen in AER2; (d) effluent N (S_{NH_x} (grey) and TN (black)); (e) effluent P (S_{IP} (grey) and TP (black)); (f) TSS in AER3; (g) methane gas production; and, (h) hydrogen sulfide gas production. Simulation time is one year. A 3-day exponential filter is used to improve visualization of the results. Raw data is presented in grey (in (a), (b), (c), (f), (g) and (h)).

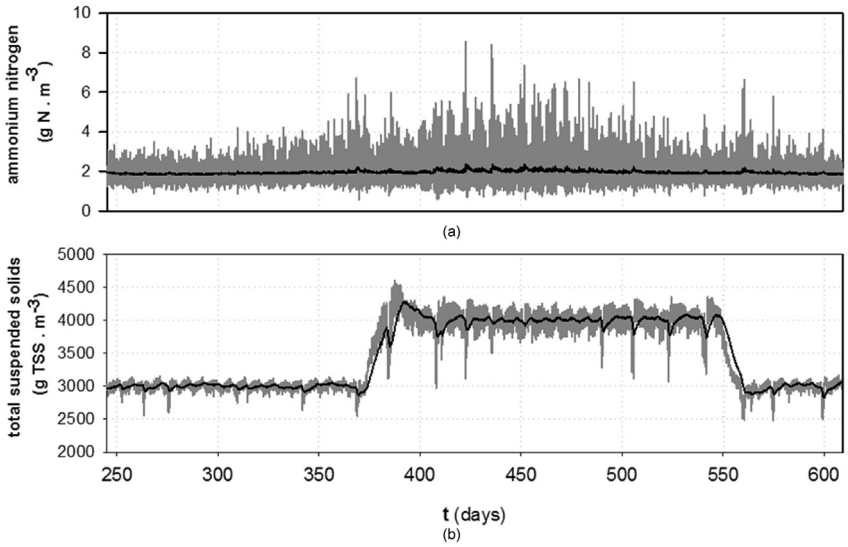

Fig. 3. Dynamic profiles (A_1) of: (a) S_{NH_x} in AER2; and, (b) X_{TSS} in AER3 after implementing alternative A_1. A 3-day exponential filter is used to improve visualization of the results. Raw data is presented in grey. (Note that T < 15 °C starts on day 357 and lasts until day 549).

3.2.1. Control strategy (A_1): cascade ammonium + wastage controller

The first alternative control strategy (A_1) is based on a cascade PI ammonium (S_{NH_x}) controller that manipulates the (S_{O_2}) set-point in AER2 (and also the airflow in AER1 and AER3 by a factor of 2.0 and 0.5, respectively) (Fig. 3a). The S_{O_2} concentration in AER2 is controlled by manipulating the air supply rate. The second controller regulates the total suspended solids (X_{TSS}) in AER3 by manipulating the wastage flow (Q_w) (Vanrolleghem et al., 2010). The set-point changes (set-point = 3000 gTSS.m^{-3} > 15 °C/4000 gTSS.m^{-3} < 15 °C) are made according to temperature (T) in order to set a longer SRT to maintain the nitrification capacity during the winter period (Fig. 3b). Additional details about the simulated control strategies can be found in Table 1. The S_{O_2} and T sensor are assumed to be close to ideal with a response time of 1 min in order to prevent unrealistic control applications. On the other hand, the S_{NH_x} sensor has a time delay of 10 min, with zero mean white noise (standard deviation of 0.5 g N.m^{-3}) (Rieger et al., 2003). The

Table 2
Evaluation criteria for the three evaluated control/operational strategies.

Operational alternatives →	Default	A_1	A_2	A_3	
$N_{Kjeldahl}$	3.5	3.6	3.6	3.7	g N.m^{-3}
N_{total}	11.2	9.2	9.1	8.5	g N.m^{-3}
P_{inorg}	5.95	2.9	0.9	0.6	g P.m^{-3}
P_{total}	6.4	3.7	1.7	1.5	g P.m^{-3}
EQI	**18 234**	**12 508**	**8237**	**7766**	kg pollution.d^{-1}
TIV S_{NH_x} (= 4 g N.m^{-3})	0.95	0.07	0.08	0.08	%
TIV N_{total} (= 14 g N.m^{-3})	0	0	0	0	%
TIV P_{total} (= 2 g P.m^{-3})	100	75	13.4	15.7	%
$E_{aeration}$	4000	3146	3218	3194	kWh.d^{-1}
$E_{production}$ [a]	5955	6054	6150	6038	kWh.d^{-1}
$SP_{disposal}$ [b]	3461	3538	3730	3487	kg TSS.d^{-1}
Q_{FeCl_3}	–	–	169	–	kg Fe.d^{-1}
$Q_{Mg(OH)_2}$	–	–	–	40	kg Mg.d^{-1}
$S_{recovered}$ [c]	–	–	–	206	kg struvite.d^{-1}
OCI [d]	**10 201**	**9495**	**13 770**	**8912**	–
G_{CH_4}	992	1009	1025	1006	kg CH_4.d^{-1}
G_{H_2S}	17.4	19.2	12.1	19.2	kg H_2S.d^{-1}
$\frac{N_{removed}}{OCI}$	0.079	0.089	0.062	0.097	kg N (removed).OCI^{-1}
$\frac{P_{removed}}{OCI}$	0.007	0.013	0.012	0.019	kg P (removed).OCI^{-1}

[a] The electricity generated by the turbine is calculated by using a factor for the energy content of the methane gas (50.014 MJ (kg CH_4)$^{-1}$) and assuming 43% efficiency for electricity generation.

[b] $SP_{disposal}$ refers to the amount of solids which accumulate in the plant over the time of evaluation combined with the amount of solids removed from the process (i.e. dewatered sludge). See Gernaey et al. (2014) for a more detailed description.

[c] $S_{recovered}$ refers to the amount of recovered struvite. See Supplemental Information for a more detailed description.

[d] Relative costs for chemicals are calculated assuming 2400 $/ton as Fe (ICIS, 2016), 600 $/ton as Mg (ICIS, 2016) and 200 $/ton as struvite (value) (Prasad and Shih, 2016; Jaffer et al., 2002; Münch and Barr, 2001).

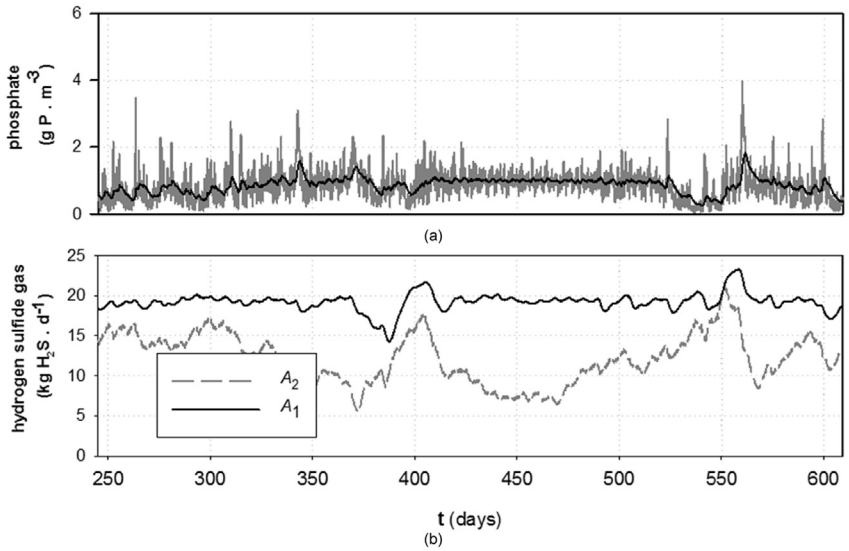

Fig. 4. Dynamic profiles (A_2) of: (a) S_{PO_4} in AER3; and, (b) G_{H_2S} in the AD after implementing alternative A_2. A 3-day exponential filter is used to improve visualization of the results. Raw data is presented in grey.

aeration system and the wastage pumping system are defined with significant dynamics assuming a response time of 4 min. Table 2 summarizes the values for the different evaluation criteria. The implementation of these controllers improves S_{PO_4} accumulation by X_{PAO} and increases nitrification/denitrification efficiency. This is mainly due to a better aeration strategy in the biological reactors. As a side effect, operational cost (*OCI*) is reduced and there is a substantial reduction of the energy consumed (see $E_{aeration}$ values in Table 2). As a further consequence, effluent quality values (N_{total}, P_{total}, *EQI*) are improved. Indeed, the open loop aeration system is highly inefficient (not sufficient during daytime and excessive at night) (see Fig. 2c). Summer/winter wasting schemes cause variations in the quantity of sludge arriving to the AD and therefore changes in the biogas production. This is translated into different potential energy recovery efficiencies (see $E_{production}$ values in Table 2).

3.2.2. Control strategy (A_2): Fe chemical precipitation in the AS section

The second alternative (A_2) involves the addition of iron (as X_{FeCl_3}, the model assumes a liquid solution of X_{FeCl_3}) in the AS section in addition to A_1 (see Table 1). The S_{PO_4} concentration in AER3 is controlled by manipulating the metal flow rate (Q_{FeCl_3}) (Fig. 4a). Additional details about the simulated control strategies can be found in Table 1. The S_{PO_4} and S_{NH_x} sensors have similar characteristics (10 min delay and zero mean white noise with a standard deviation of 0.5 g P or N.m^{-3}). Response time for Q_{FeCl_3} is also 10 min (avoiding unrealistic control actions).

Results reported in Table 2 show a reduction in P_{inorg}, time in violation (*TIV*) P_{total} as well as the *EQI* due to chemical P precipitation (see Figs. 2e and 4a, respectively). On the other hand, there is an increase in sludge production (SP_{total}) and the *OCI* as a trade-off. The aeration energy ($E_{aeration}$) also slightly increase from scenario A_1 to A_2 mainly due to reduced PAO activity brought about by chemical phosphorus removal; less organics are taken up by in the anaerobic part of the activated sludge unit in scenario A_2 and, as a consequence, more organics need to be oxidized in the aerobic part. It is important to highlight the additional beneficial effect of X_{FeCl_3} addition in the sludge line. Indeed, under anaerobic conditions hydrous ferric oxides (X_{HFO-H}, X_{HFO-L}) are chemically reduced to Fe (II) ($S_{Fe^{2+}}$) using hydrogen(S_{H_2}) and/or sulfides (S_{IS}) as electron donors. Also, iron phosphates ($X_{HFO-H,P}$, $X_{HFO-L,P}$) formed in the activated sludge process water line might re-dissolve under anaerobic conditions in the digesters to precipitate with sulfide (X_{FeS}). This is due to the much lower solubility of iron sulfide as compared to iron phosphate (Stumm and Morgan, 1996). The control strategy reduces undesirable inhibition/odour/corrosion problems, as well as risks for human health, as indicated by the higher G_{CH_4} and lower G_{H_2S} values compared to (A_1) (see Figs. 2h and 4b, respectively). Similar conclusions were reached by the experimental campaigns/measurements run by Mamais et al. (1994), Ge et al. (2013) and Zhang et al. (2013).

It is important to highlight that the addition of Fe substantially changes the whole P and S cycle through the entire plant while N fluxes are barely affected. The fraction of P sent to the sludge line is increased from 51 to 67% (94–127 kg P.day^{-1}) (mainly as $X_{HFO-H,P}$, $X_{HFO-L,P}$, $X_{HFO-H,P,old}$, $X_{HFO-L,P,old}$) (see Fig. SS2 in Supplemental Information). This Fe addition reduces the quantity of $X_{Ca_3(PO_4)_2}$ and $X_{MgNH_4PO_4}$ formed in the AD which, from a practical point of view, leads to less problems with their deposition in the pipes. Similar findings are also found in the following studies: Luedecke et al. (1989); Doyle and Parsons (2002) and Mamais et al. (1994). When it comes to S, there is a substantial reduction of the quantity of Z_{H_2S} in the AD due to the preferential binding with Fe (from 5100 to 4400 ppm). As a result, there is a lower quantity of H_2S in the gas phase and therefore the quantity of S leaving the plant via sludge disposal (as precipitate X_{FeS}) increases. There is a slight decrease of pH due to the increase of the contra-ion Cl^- added as part of the iron precipitation.

3.2.3. Control strategy (A_3): potential P recovery as struvite in the digester supernatant

The last alternative implies a modification of the original plant layout by adding a stripping unit (STRIP) for pH increase, a crystallizer (CRYST) to facilitate struvite recovery, a magnesium hydroxide dosage tank ($X_{Mg(OH)_2}$) and a dewatering unit (DEW2) for potential P recovery (Kazadi Mbamba et al., 2016). The assumed hydraulic retention times (HRT) of the STRIP and CRYST units are approximately 2 h and 18 h, respectively (Tchobanoglous et al., 2003). Fig. SS3 (in Supplemental Information) shows the effect of

the extra units on the total P fluxes. Simulation results indicate that the quantity of returning N and P from the AD supernatant is reduced from 221 to 201 kg N.day^{-1} and 30 to 1.3 kg P.day^{-1}, respectively (as a result of recovering P as $X_{MgNH_4PO_4}$). The latter leads to a reduction of the nutrient load to be treated in the biological reactor and decreases the quantity of P lost in the effluent (from 96 to 60 kg P.day^{-1}). When this is translated to evaluation indices (Table 2), a substantial reduction in the effluent related criteria (N_{total}, P_{total}, *EQI*) can be seen. The *OCI* is lower compared to A_2 due to: (1) the lower price of magnesium hydroxide ($X_{Mg(OH)_2}$) compared to iron chloride (X_{FeCl_3}); and, (2) the potential economic benefit resulting from selling struvite ($X_{MgNH_4PO_4}$).

Additional simulations show that these values can be modified by changing the airflow ($Q_{stripping}$) and the chemical dosage ($Q_{Mg(OH)_2}$) in the stripping unit. At high airflows ($Q_{stripping}$) the quantity of Z_{CO_2} stripped increases and consequently the pH (CO_2 has acidifying behaviour) (Fig. 5a, h). The latter favours struvite ($X_{MgNH_4PO_4}$) precipitation (Fig. 5b, g). A higher quantity of Mg ($Q_{Mg(OH)_2}$) also drives the pH higher (Fig. 5a, f). These results show that $X_{MgNH_4PO_4}$ precipitation is mainly limited by $Z_{Mg^{2+}}$ rather than $Z_{NH_4^+}$ and $Z_{PO_4^{3-}}$. This explains the substantial increase of $X_{MgNH_4PO_4}$ when the quantity of Mg is higher (note that an overdose of magnesium is also not beneficial due to possible precipitation of dolomite, etc.). The latter has an effect on P in the AD supernatant (Fig. 5e) and consequently the *EQI* (Fig. 5c). High $Q_{Mg(OH)_2}$ decreases the *OCI* since the struvite ($X_{MgNH_4PO_4}$) is accounted for as a potential benefit (Fig. 5d). Above the P/Mg stoichiometric ratios, additional Mg is just increasing the cost without further benefit, $Q_{Mg(OH)_2}$ > 40 kg Mg.day^{-1}. Fig. 5e, f, g and h show the dynamic profiles of pH at different $Q_{stripping}/Q_{Mg(OH)_2}$. One might notice the effect that the X_{TSS} controller has on the quantity of sludge leaving the AD as a result of changing the TSS set-point in AER3.

3.2.4. Environmental/economic evaluation summary

In all cases, the proposed alternatives (A_1, A_2, A_3) result in substantial improvements with respect to the open loop default configuration (A_0). The implementation of a better aeration strategy and time-varying sludge wasting scheme (A_1) results in a favourable alternative. Simulation results show that this option leads to larger N and P effluent reductions, but also a more cost-effective way to operate the plant. Both A_2 and A_3 substantially reduce the quantity of effluent P. The main difference between the two relies on that A_3 implies a major modification of the plant layout. Capital expenditures of the CRYST, STRIP, blowers, civil, electrical and piping works should be included in order to make a more complete assessment. In contrast, alternative A_2 can be arranged easily with an extra dosing tank. Even though the potential benefit that comes from struvite ($S_{recovered}$) recovery is very uncertain and these results should be taken with care (Shu et al., 2006; Vaneeckhaute et al., 2017), the cost for each kg N and P removed is much higher for A_2 (see $N_{removed}/OCI$ and $P_{removed}/OCI$ values in Table 2). The latter means that the cost is dramatically lower for A_3 and payback time for the new installation should be short. It is important to highlight that a thorough economic study is

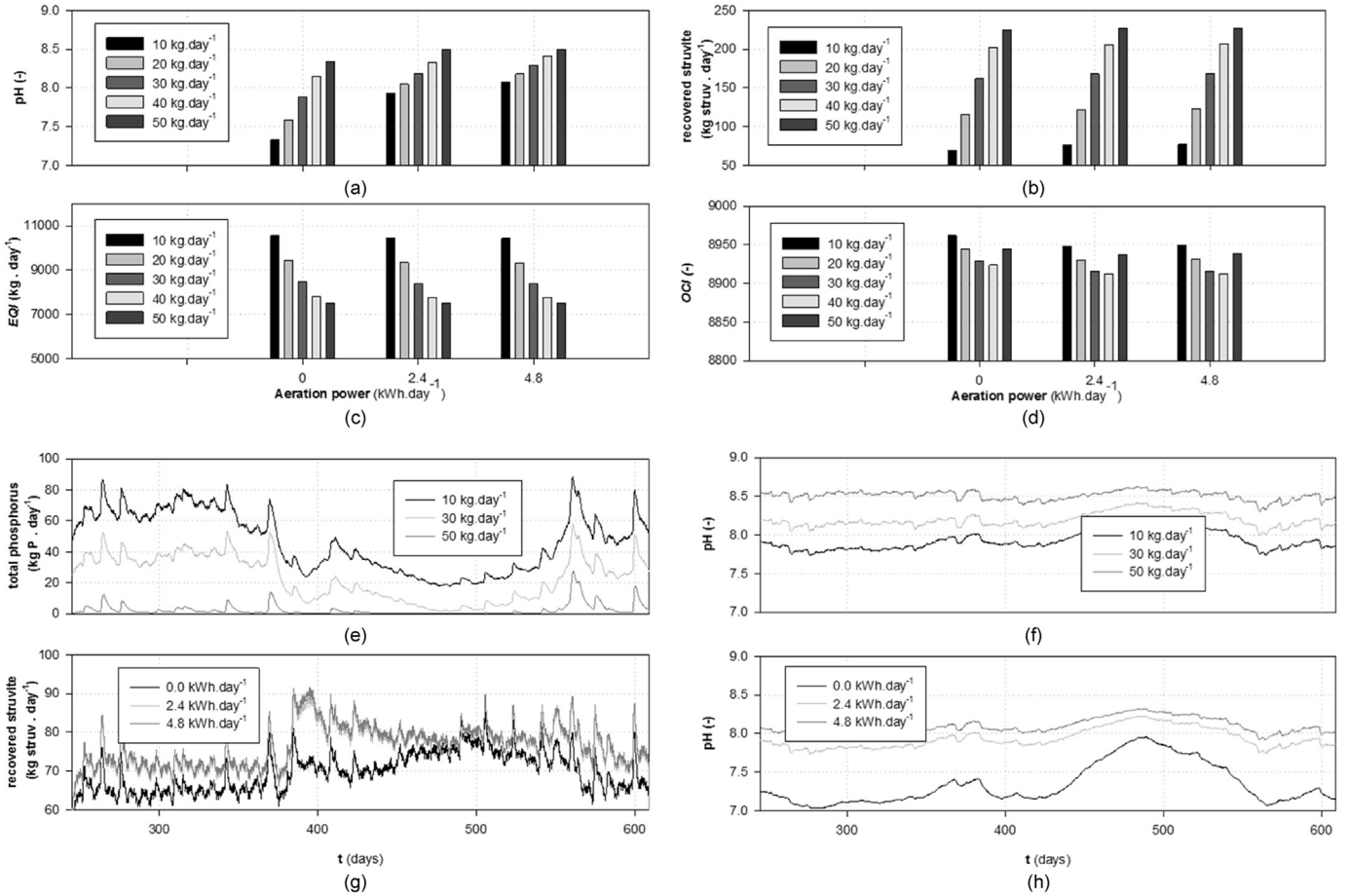

Fig. 5. Effect of aeration power $Q_{stripping}$ /dosage addition $Q_{Mg(OH)_2}$ on (a), (f), (h): pH in the stripping unit (STRIP); (b), (g): quantity of recovered struvite; (c) EQI; (d) OCI; and, (e) P content in the anaerobic digester supernatant. A 3-day exponential filter is used to improve visualization of the results in (e), (f), (g) and (h).

not carried out in this paper since it is not within the scope of the study.

4. Challenges and limitations of the proposed approach

The model results presented in this paper demonstrate the effects that different operational modes might have on the physico-chemical and biological transformations of P in a WRRF. The observations noted above also suggest the importance of linking the P with the S and Fe cycles since this paper identifies that potential control strategies not only address the primary goal, but have an effect that is cycled throughout the process (see Fig. 1, Fig. SS2). This is critical to enable the development, testing and evaluation of phosphorus control/recovery strategies in the context of water resource recovery facilities (Jeppsson et al., 2013). In the following section, we discuss the applicability of the model assumptions made to describe P, S and Fe interactions, the suitability of the number of considered processes and some practical implications for plant-wide modelling/development of resource recovery strategies.

4.1. Selection of the relevant process and interpretation of the results

The model presented in this paper accounts for some of the most important factors affecting the P, S and Fe cycles in a wastewater treatment facility (Batstone et al., 2015). Additional processes may be added to consider novel control strategies. For example, sulfide can be directly controlled in the digester through microaeration, which converts sulfide to elemental sulfur (Krayzelova et al., 2015). The approach taken in this paper in describing sulfide oxidation to elemental sulfur in the anaerobic zone of the activated sludge process is directly applicable to this problem.

When it comes to P recovery, important assumptions were made in order to run the third alternative (A_3). For example, calcium precipitation is not assumed in the crystallizer. This is due to the low amounts of calcium in this scenario, and because calcium generally complexes with carbonate (Kazadi Mbamba et al., 2015a). In high-calcium (hard) waters, it may become critical. Another important factor is that ideal solids separation in the crystallizer is assumed. This will depend on the specific implementation of the crystallizer and crystal recovery. Precipitate dissolution (and particularly Mg dissolution) is currently simplified. The latter may have an important effect on the overall process performance (Romero-Güiza et al., 2015). In the water line, competition between PAO and Glycogen Accumulating Organisms (GAO) (Lopez-Vazquez et al., 2007, 2009; Oehmen et al., 2010) is not accounted for. This may have a strong influence on the overall biological P removal. S and Fe oxidation processes have been modelled chemically, but there are numerous studies demonstrating that these processes are also biologically mediated (Xu et al., 2013). In any case, the oxidation processes goes to completion. This may have limited impact on the overall process, due to the ubiquitous capability of sulfur oxidation/reduction capability in heterotrophic organisms.

The alternating aerated/non-aerated periods might promote the formation of nitrous oxide gases (Ni et al., 2014; Ni and Yuan, 2015; Lindblom et al., 2016). When evaluating the suitability of different control/operational strategies, this factor is not included in the study, and if it was, it might partly change the overall discussion of the results (Flores-Alsina et al., 2014a; Sweetapple et al., 2014; Mannina et al., 2016). Closely related to that, it is important to point out that aeration energy could be better estimated with a more detailed piping/distribution model (Beltrán et al., 2011). In addition, the aeration model could be further improved using a detailed mass transfer model which might change the quantity of stripped gas (that might be overestimated with the current model) (Lizarralde et al., 2015). All these options, including evaluating the impact of influent flow equalization basins, are identified as promising research avenues that will be further studied in the near future (Jeppsson et al., 2013). The latter could be combined with proper electricity tariff models (Aymerich et al., 2015) and dramatically change the way how energy must be optimized. In this case study relative costs have been used (Jeppsson et al., 2007) due to the volatility of the prices (chemicals, electricity, sludge disposal, …). Proper cost estimates and variations (uncertainty ranges) will provide customized solutions for a particular case.

4.2. General applicability of the presented model

Even though the shown numeric results are case-specific, the presented tools are generally applicable, and an earlier version has been successfully applied to a real plant (Kazadi Mbamba et al., 2016). The influent characteristics (Gernaey et al., 2011) can be scaled to different situations (Flores-Alsina et al., 2014b; Snip et al., 2014; Snip et al., 2016; Kazadi Mbamba et al., 2016). The original BSM2 (only carbon and nitrogen) plant has been adapted to simulate the dynamics of some Swedish plants (Arnell et al., 2013). The ASM2d and ADM1 (separately) have been applied to multiple case studies successfully describing plant dynamics (Gernaey and Jørgensen, 2004; Batstone et al., 2015). The P principles upon which the new AD model is constructed are experimentally validated in different studies (Ikumi et al., 2011; Wang et al., 2016). The same applies to the S module in both AS (Gutierrez et al., 2010) and AD (Batstone, 2006; Barrera et al., 2015) models. As stated above, expansion to consider cases such as microaeration in anaerobic digesters can be done through direct adaptation of the approach taken in the activated sludge process.

The model may also be applied to integrated urban water systems, wherein, chemicals added/present in the sewer network or during drinking water production may have an impact on the downstream wastewater treatment processes (particularly for systems where there is no primary sedimentation) (Pikaar et al., 2014; Nielsen et al., 2005; Ge et al., 2013).

4.3. Optimization tool for resource recovery

The described approach has strong potential for optimizing resource recovery (i.e. biogas and phosphorus recovery) in a plant-wide context, and possibly also in the larger sewage catchment. For example, the potential energy/financial benefits of an improved biogas production can be balanced with the addition of selected chemicals (Flores-Alsina et al., 2016) or substrates for co-digestion (Arnell et al., 2016). Another potential option is P recovery (Vaneeckhaute, 2015). Results presented in Section 3.2.3 show that the total quantity of recovered P is rather small (31.8 kg $P.d^{-1}$/196.6 kg $P.d^{-1}$). This is mainly due to the different P losses/transformations through the different units in the plant. Different operational conditions (Marti et al., 2008, 2010; Latif et al., 2015) could reduce the quantity of P lost in the effluent, could minimize uncontrolled phosphorus precipitation in the anaerobic digester and enhance phosphorus recovery in the crystallizer. In a similar way, smarter dosing strategies (similarly to A_2) could be evaluated in order to reduce the use of chemicals and to adapt to changes in the P loads due to operational changes (summer/winter). Airflow in the stripping unit could be adjusted in order to reach a desired pH (feedback controller).

5. Conclusions

The main findings of this study are summarized in the following points:

1) A plant-wide model describing the main P transformations and the close interactions with the S and Fe cycles in wastewater treatment systems is presented;
2) Operational conditions have a strong effect on the fate of P compounds: accumulation by X_{PAO}, adsorption into Fe ($X_{HFO-H,P}$, $X_{HFO-L,P}$) and co-precipitation with different metals ($X_{HFO-H,P,old}$, $X_{HFO-L,P,old}$, $X_{Ca_3(PO_4)_2}$, $X_{MgNH_4PO_4}$);
3) Overall and individual mass balances quantify the distribution of P (as well as N, S and Fe) in both water and sludge line;
4) The set of models presented in this study makes up a useful engineering tool to aid decision makers/wastewater engineers when upgrading/improving the sustainability and efficiency of wastewater treatment systems (e.g. reduce consumption and increase recovery).

6. Software availability

The MATLAB/SIMULINK code of the models presented in this paper is available upon request, including the implementation of the physico-chemical and biological modelling framework in BSM2. Using this code, interested readers will be able to reproduce the results summarized in this study. To express interest, please contact Dr. Ulf Jeppsson (ulf.jeppsson@iea.lth.se) at Lund University (Sweden), Prof. Krist V. Gernaey (kvg@kt.dtu.dk) or Dr. Xavier Flores-Alsina (xfa@kt.dtu.dk) at the Technical University of Denmark (Denmark) or Prof. Damien Batstone (damienb@awmc.uq.edu.au) at The University of Queensland (Australia).

Acknowledgements

Ms Solon and Dr Flores-Alsina acknowledge the Marie Curie Program of the EU 7th Framework Programme FP7/2007–2013 under REA agreement 289193 (SANITAS) and 329349 (PROTEUS), respectively. Dr Flores-Alsina gratefully acknowledges the financial support of the collaborative international consortium WATER-JPI2015 WATINTECH (Reference ID 196) of the Water Challenges for a Changing World Joint Programming Initiative (Water JPI) 2015 call. Parts of this research were developed during the research stay of Dr Flores-Alsina at the Department of Civil Engineering at the University of Cape Town (South Africa) and at the Advanced Water Management Centre at The University of Queensland (Australia) and also developed during the short term scientific COST mission (STSM, COST Water2020) of Ms Solon at the Biosystems Control research unit at the Department of Biosystems Engineering at Ghent University (Belgium). The research was supported financially by The University of Queensland through the UQ International Scholarships (UQI). Peter Vanrolleghem holds the Canada Research Chair in Water Quality Modelling. Dr. Stephan Tait at the Advanced Water Management Centre at The University of Queensland (Australia) and Chris Brouckaert at the Pollution Research Group at the University of KwaZulu-Natal are acknowledged for their valuable contributions on the discussions during the model development. The International Water Association (IWA) is also acknowledged for their promotion of this collaboration through their sponsorship of the IWA Task Group on Generalized Physico-chemical Modelling Framework (PCM). A concise version of this paper was presented at Watermatex 2015 (Gold Coast, Australia, June 2015).

Appendix A. Supplementary data

Supplementary data related to this article can be found at http://dx.doi.org/10.1016/j.watres.2017.02.007.

References

Arnell, M., Astals, S., Åmand, L., Batstone, D.J., Jensen, P.D., Jeppsson, U., 2016. Modelling anaerobic co-digestion in Benchmark Simulation Model No. 2: parameter estimation, substrate characterisation and plant-wide integration. Water Res. 98, 138–146.
Arnell, M., Sehlen, R., Jeppsson, U., 2013. Practical use of wastewater treatment modelling and simulation as a decision support tool for plant operators—case study on aeration control at Linköping wastewater treatment plant. In: Proceedings of the 13th Nordic Wastewater Conference, Malmö, Sweden, 8–10 October 2013.
Aymerich, I., Rieger, L., Sobhani, R., Rosso, D., Corominas, L., 2015. The difference between energy consumption and energy cost: modelling energy tariff structures for water resource recovery facilities. Water Res. 81, 113–123.
Barat, R., Montoya, T., Seco, A., Ferrer, J., 2011. Modelling biological and chemically induced precipitation of calcium phosphate in enhanced biological phosphorus removal systems. Water Res. 45 (12), 3744–3752.
Barat, R., Serralta, J., Ruano, V., Jimenez, E., Ribes, J., Seco, A., Ferrer, J., 2013. Biological Nutrient Removal no 2 (BNRM2): a general model for wastewater treatment plants. Water Sci. Technol. 67 (7), 1481–1489.
Barker, P.S., Dold, P.L., 1997. General model for biological nutrient removal activated-sludge systems: model presentation. Water Environ. Res. 69 (5), 969–984.
Barrera, E.L., Spanjers, H., Solon, K., Amerlinck, Y., Nopens, I., Dewulf, J., 2015. Modeling the anaerobic digestion of cane-molasses vinasse: extension of the Anaerobic Digestion Model No. 1 (ADM1) with sulfate reduction for a very high strength and sulfate rich wastewater. Water Res. 71, 42–54.
Batstone, D.J., 2006. Mathematical modelling of anaerobic reactors treating domestic wastewater: rational criteria for model use. Rev. Environ. Sci. Biotechnol. 5, 57–71.
Batstone, D.J., Keller, J., Angelidaki, I., Kalyuzhnyi, S.V., Pavlostathis, S.G., Rozzi, A., Sanders, W.T.M., Siegrist, H., Vavilin, V.A., 2002. Anaerobic Digestion Model No. 1. IWA Scientific and Technical Report No. 13. IWA Publishing, London, UK.
Batstone, D.J., Puyol, D., Flores-Alsina, X., Rodriguez, J., 2015. Mathematical modelling of anaerobic digestion processes: applications and future needs. Rev. Environ. Sci. Biotechnol. 14 (4), 595–613.
Beltrán, S., Logrono, C., Maiza, M., Ayesa, E., 2011. Model based optimization of aeration system in WWTP. In: Proceedings of Watermatex2011, San Sebastian, Spain, 20–22 June 2011.
Copp, J.B. (Ed.), 2002. The COST Simulation Benchmark – Description and Simulator Manual. Office for Official Publications of the European Communities, Luxembourg, ISBN 92-894-1658-0.
de Gracia, M., Sancho, L., García-Heras, J.L., Vanrolleghem, P., Ayesa, E., 2006. Mass and charge conservation check in dynamic models: application to the new ADM1 model. Water Sci. Technol. 53 (1), 225–240.
Doyle, J.D., Parsons, S.A., 2002. Struvite formation, control and recovery. Water Res. 36 (16), 3925–3940.
Ekama, G.A., 2009. Using bioprocess stoichiometry to build a plant-wide mass balance based steady-state WWTP model. Water Res. 43 (8), 2101–2120.
Ekama, G.A., Barnard, J.L., Gunthert, F.W., Krebs, P., McCorquodale, J.A., Parker, D.S., Wahlberg, E.J., 1997. Secondary Settling Tanks: Theory, Modelling, Design and Operation. IWA Publishing, London, UK. IWA Scientific and Technical Report No. 6.
Ekama, G.A., Wentzel, M.C., 2004. A predictive model for the reactor inorganic suspended solids concentration in activated sludge systems. Water Res. 38 (8), 4093–4106.
Ekama, G.A., Wentzel, M.C., Sötemann, S.W., 2006. Tracking the inorganic suspended solids through biological treatment units of wastewater treatment plants. Water Res. 40 (19), 3587–3595.
Fedorovich, V., Lens, P., Kalyuzhnyi, S., 2003. Extension of anaerobic digestion model No. 1 with processes of sulfate reduction. Appl. Biochem. Biotechnol. 109, 33–45.
Flores-Alsina, X., Arnell, M., Amerlinck, Y., Corominas, L., Gernaey, K.V., Guo, L., Lindblom, E., Nopens, I., Porro, J., Shaw, A., Snip, L., Vanrolleghem, P.A., Jeppsson, U., 2014a. Balancing effluent quality, economical cost and greenhouse gas emissions during the evaluation of plant-wide wastewater treatment plant control strategies. Sci. Total Environ. 466–467, 616–624.
Flores-Alsina, X., Gernaey, K.V., Jeppsson, U., 2012. Benchmarking biological nutrient removal in wastewater treatment plants: influence of mathematical model assumptions. Water Sci. Technol. 65 (8), 1496–1505.
Flores-Alsina, X., Kazadi Mbama, C., Solon, K., Vrecko, D., Tait, S., Batstone, D., Jeppsson, U., Gernaey, K.V., 2015. A plant-wide aqueous phase chemistry module describing pH variations and ion speciation/pairing in wastewater treatment models. Water Res. 85, 255–265.
Flores-Alsina, X., Saagi, R., Lindblom, E., Thirsing, C., Thornberg, D., Gernaey, K.V., Jeppsson, U., 2014b. Calibration and validation of a phenomenological influent pollutant disturbance scenario generator using full-scale data. Water Res. 51, 172–185.
Flores-Alsina, X., Solon, K., Kazadi Mbamba, C., Tait, S., Jeppsson, U., Gernaey, K.V., Batstone, D.J., 2016. Modelling phosphorus, sulphur and iron interactions during the dynamic simulation of anaerobic digestion processes. Water Res. 95, 370–382.
Ge, H., Zhang, L., Batstone, D.J., Keller, J., Yuan, Z., 2013. Impact of iron salt dosage to sewers on downstream anaerobic sludge digesters: sulfide control and methane production. J. Environ. Eng. 139, 594–601.

Gernaey, K.V., Flores-Alsina, X., Rosen, C., Benedetti, L., Jeppsson, U., 2011. Dynamic influent pollutant disturbance scenario generation using a phenomenological modelling approach. Environ. Model. Softw. 26 (11), 1255–1267.
Gernaey, K.V., Jeppsson, U., Batstone, D.J., Ingildsen, P., 2006. Impact of reactive settler models on simulated WWTP performance. Water Sci. Technol. 53 (1), 159–167.
Gernaey, K.V., Jeppsson, U., Vanrolleghem, P.A., Copp, J.B., 2014. Benchmarking of Control Strategies for Wastewater Treatment Plants. IWA Publishing, London, UK. IWA Scientific and Technical Report No. 23.
Gernaey, K.V., Jørgensen, S.B., 2004. Benchmarking combined biological phosphorus and nitrogen removal wastewater treatment processes. Control Eng. Pract. 12 (3), 357–373.
Grau, P., Copp, J., Vanrolleghem, P.A., Takács, I., Ayesa, E., 2009. A comparative analysis of different approaches for integrated WWTP modelling. Water Sci. Technol. 59 (1), 141–147.
Grau, P., de Gracia, M., Vanrolleghem, P.A., Ayesa, E., 2007. A new plant-wide modelling methodology for WWTPs. Water Res. 41 (19), 4357–4372.
Gutierrez, O., Park, D., Sharma, K.R., Yuan, Z., 2010. Iron salts dosage for sulfide control in sewers induces chemical phosphorus removal during wastewater treatment. Water Res. 44 (11), 3467–3475.
Guerrero, J., Flores-Alsina, X., Guisasola, A., Baeza, J.A., Gernaey, K.V., 2013. Effect of nitrite, limited reactive settler and plant design configuration on the predicted performance of a simultaneous C/N/P removal WWTP. Bioresour. Technol. 136, 680–688.
Harding, T.H., Ikumi, D.S., Ekama, G.A., 2011. Incorporating phosphorus into plant wide wastewater treatment plant modelling anaerobic digestion. In: Proceedings of Watermatex2011, San Sebastian, Spain, 20–22 June 2011.
Hauduc, H., Rieger, L., Takács, I., Héduit, A., Vanrolleghem, P.A., Gillot, S., 2010. A systematic approach for model verification: application on seven published activated sludge models. Water Sci. Technol. 61 (4), 825–839.
Hauduc, H., Takács, I., Smith, S., Szabo, A., Murthy, S., Daigger, G.T., Spérandio, M., 2015. A dynamic physicochemical model for chemical phosphorus removal. Water Res. 73, 157–170.
Henze, M., Gujer, W., Mino, T., van Loosdrecht, M.C.M., 2000. Activated Sludge Models ASM1, ASM2, ASM2d, and ASM3. IWA Publishing, London, UK. IWA Scientific and Technical Report No. 9.
Henze, M., van Loosdrecht, M.C.M., Ekama, G.A., 2008. Biological Wastewater Treatment: Principles, Modeling, and Design. IWA Publishing, London, UK.
ICIS, 2016. Indicative Chemical Prices A-z. Retrieved from. http://www.icis.com/chemicals/channel-info-chemicals-a-z/ [Accessed 14 06 2016].
Ikumi, D.S., Brouckaert, C.J., Ekama, G.A., 2011. Modelling of struvite precipitation in anaerobic digestion. In: Proceedings of Watermatex2011, San Sebastian, Spain, 20–22 June 2011.
Ikumi, D.S., Harding, T.H., Ekama, G.A., 2014. Biodegradability of wastewater and activated sludge organics in anaerobic digestion. Water Res. 56 (1), 267–279.
Jaffer, Y., Clark, T.A., Pearce, P., Parsons, S.A., 2002. Potential phosphorus recovery by struvite formation. Water Res. 36 (7), 1834–1842.
Jeppsson, U., Alex, J., Batstone, D., Benedetti, L., Comas, J., Copp, J.B., Corominas, L., Flores-Alsina, X., Gernaey, K.V., Nopens, I., Pons, M.-N., Rodriguez-Roda, I., Rosen, C., Steyer, J.-P., Vanrolleghem, P.A., Volcke, E.I.P., Vrecko, D., 2013. Benchmark simulation models, quo vadis? Water Sci. Technol. 68 (1), 1–15.
Jeppsson, U., Pons, M.N., Nopens, I., Alex, J., Copp, J.B., Gernaey, K.V., Rosen, C., Steyer, J.P., Vanrolleghem, P.A., 2007. Benchmark Simulation Model No 2 – general protocol and exploratory case studies. Water Sci. Technol. 56 (8), 287–295.
Kazadi Mbamba, C., Flores-Alsina, X., Batstone, D.J., Tait, S., 2015a. A generalised chemical precipitation modelling approach in wastewater treatment applied to calcite. Water Res. 68, 342–353.
Kazadi Mbamba, C., Flores-Alsina, X., Batstone, D.J., Tait, S., 2015b. A systematic study of multiple minerals precipitation modelling in wastewater treatment. Water Res. 85, 359–370.
Kazadi Mbamba, C., Flores-Alsina, X., Batstone, D.J., Tait, S., 2016. Validation of a plant-wide modelling approach with minerals precipitation in a full-scale WWTP. Water Res. 100, 169–183.
Krayzelova, L., Bartacek, J., Díaz, I., Jeison, D., Volcke, E.I.P., Jenicek, P., 2015. Microaeration for hydrogen sulfide removal during anaerobic treatment: a review. Rev. Environ. Sci. Biotechnol. 14 (4), 703–725.
Latif, M.A., Mehta, C.M., Batstone, D.J., 2015. Low pH anaerobic digestion of waste activated sludge for enhanced phosphorous release. Water Res. 81, 288–293.
Lizarralde, I., Fernandez-Arevalo, T., Brouckaert, C., Vanrolleghem, P.A., Ikumi, D., Ekama, D., Ayesa, E., Grau, P., 2015. A new general methodology for incorporating physico-chemical transformations into multiphase wastewater treatment process models. Water Res. 74, 239–256.
Lindblom, E., Arnell, M., Flores-Alsina, X., Stenström, F., Gustavsson, D.J.I., Yang, J., Jeppsson, U., 2016. Dynamic modelling of nitrous oxide emissions from three Swedish sludge liquor treatment systems. Water Sci. Technol. 73 (4), 798–806.
Lopez-Vazquez, C.M., Hooijmans, C.M., Brdjanovic, D., Gijzen, H.J., van Loosdrecht, M.C.M., 2007. A practical method for quantification of phosphorus- and glycogen-accumulating organism populations in activated sludge systems. Water Environ. Res. 79 (13), 2487–2498.
Lopez-Vazquez, C.M., Oehmen, A., Hooijmans, C.M., Brdjanovic, D., Gijzen, H.J., Yuan, Z., van Loosdrecht, M.C.M., 2009. Modeling the PAO-GAO competition: effects of carbon source, pH and temperature. Water Res. 43 (2), 450–462.
Luedecke, C., Hermanowicz, S.W., Jenkins, D., 1989. Precipitation of ferric phosphate in activated sludge: a chemical model and its verification. Water Sci. Technol. 21 (4–5), 325–337.
Mamais, D., Pitt, P.A., Cheng, Y.W., Loiacono, J., Jenkins, D., 1994. Determination of ferric chloride dose to control struvite precipitation in anaerobic sludge digesters. Water Environ. Res. 66 (7), 912–918.
Mannina, G., Ekama, G., Caniani, D., Cosenza, A., Esposito, G., Gori, R., Garrido-Baserba, M., Rosso, D., Olsson, G., 2016. Greenhouse gases from wastewater treatment - a review of modelling tools. Sci. Total Environ. 551, 254–270.
Marti, N., Pastor, L., Bouzas, A., Ferrer, J., Seco, A., 2010. Phosphorus recovery by struvite crystallization in WWTPs: influence of the sludge treatment line operation. Water Res. 44 (7), 2371–2379.
Marti, N., Ferrer, J., Seco, A., Bouzas, A., 2008. Optimization of sludge line management to enhance phosphorus recovery in WWTP. Water Res. 42 (18), 4609–4618.
Martin, C., Vanrolleghem, P.A., 2014. Analysing, completing, and generating influent data for WWTP modelling: a critical review. Environ. Model. Softw. 60, 188–201.
Münch, E.V., Barr, K., 2001. Controlled struvite crystallisation for removing phosphorus from anaerobic digester sidestreams. Water Res. 35 (1), 151–159.
Musvoto, E.V., Wentzel, M.C., Ekama, G.A., 2000. Integrated chemical-physical processes modelling - II. Simulating aeration treatment of anaerobic digester supernatants. Water Res. 34 (6), 1868–1880.
Ni, B.J., Peng, L., Law, Y., Guo, J., Yuan, Z., 2014. Modeling of nitrous oxide production by autotrophic ammonia-oxidizing bacteria with multiple production pathways. Environ. Sci. Technol. 48 (7), 3916–3924.
Ni, B.J., Yuan, Z., 2015. Recent advances in mathematical modeling of nitrous oxides emissions from wastewater treatment processes. Water Res. 87, 336–346.
Nielsen, A.H., Lens, P., Vollertsen, J., Hvitved-Jacobsen, T., 2005. Sulfide–iron interactions in domestic wastewater from a gravity sewer. Water Res. 39 (12), 2747–2755.
Nopens, I., Batstone, D.J., Copp, J.B., Jeppsson, U., Volcke, E., Alex, J., Vanrolleghem, P.A., 2009. An ASM/ADM model interface for dynamic plant-wide simulation. Water Res. 43 (7), 1913–1923.
Nopens, I., Benedetti, L., Jeppsson, U., Pons, M.-N., Alex, J., Copp, J.B., Gernaey, K.V., Rosen, C., Steyer, J.-P., Vanrolleghem, P.A., 2010. Benchmark Simulation Model No 2 – finalisation of plant layout and default control strategy. Water Sci. Technol. 62 (9), 1967–1974.
Oehmen, A., Lopez-Vazquez, C.M., Carvalho, G., Reis, M.A.M., van Loosdrecht, M.C.M., 2010. Modelling the population dynamics and metabolic diversity of organisms relevant in anaerobic/anoxic/aerobic enhanced biological phosphorus removal processes. Water Res. 44 (15), 4473–4486.
Otterpohl, R., Freund, M., 1992. Dynamic models for clarifiers of activated sludge plants with dry and wet weather flows. Water Sci. Technol. 26 (5–6), 1391–1400.
Pikaar, I., Sharma, K.R., Hu, S., Gernjak, W., Keller, J., Yuan, Z., 2014. Reducing sewer corrosion through integrated urban water management. Science 345 (6198), 812–814.
Pokorna-Krayzelova, L., Mampaey, K.E., Vannecke, T.P.W., Bartacek, J., Jenicek, P., Volcke, E.I.P., 2017. Model-based Optimization of Microaeration for Biogas Desulfurization in UASB Reactors submitted for publication.
Prasad, M.N.V., Shih, K., 2016. Environmental Materials and Waste: Resource Recovery and Pollution Prevention. Elsevier Inc, London, UK.
Rieger, L., Alex, J., Winkler, S., Boehler, M., Thomann, M., Siegrist, H., 2003. Progress in sensor technology - progress in process control Part I: sensor property investigation and classification. Water Sci. Technol. 47 (2), 103–112.
Romero-Güiza, M.S., Tait, S., Astals, S., Del Valle-Zermeño, R., Martínez, M., Mata-Alvarez, J., Chimenos, J.M., 2015. Reagent use efficiency with removal of nitrogen from pig slurry via struvite: a study on magnesium oxide and related by-products. Water Res. 84, 286–294.
Rosen, C., Vrecko, D., Gernaey, K.V., Pons, M.-N., Jeppsson, U., 2006. Implementing ADM1 for plant-wide benchmark simulations in Matlab/Simulink. Water Sci. Technol. 54 (4), 11–19.
Ruano, M.V., Serralta, J., Ribes, J., Garcia-Usach, F., Bouzas, A., Barat, R., 2011. Application of the general model Biological Nutrient Removal Model No. 1 to upgrade two full-scale WWTPs. Environ. Technol. 33 (9), 1005–1012.
Serralta, J., Borras, L., Seco, A., 2004. An extension of ASM2d including pH calculation. Water Res. 38 (19), 4029–4038.
Shu, L., Schneider, P., Jegatheesan, V., Johnson, J., 2006. An economic evaluation of phosphorus recovery as struvite from digester supernatant. Bioresour. Technol. 97 (17), 2211–2216.
Siegrist, H., Brunner, I., Koch, G., Con Phan, L., Van Chieu, L., 1999. Reduction of biomass decay under anoxic and anaerobic conditions. Water Sci. Technol. 39 (1), 129–137.
Skogestad, S., 2000. Plantwide control: the search for the self-optimizing control structure. J. Process Control 10, 487–507.
Snip, L., Flores-Alsina, X., Plósz, B.G., Jeppsson, U., Gernaey, K.V., 2014. Modelling the occurrence, transport and fate of pharmaceuticals in wastewater systems. Environ. Model. Softw. 62, 112–127.
Snip, L.J.P., Flores-Alsina, X., Aymerich, I., Rodríguez-Mozaz, S., Barceló, D., Plósz, B.G., Corominas, L., Rodriguez-Roda, I., Jeppsson, U., Gernaey, K.V., 2016. Generation of synthetic data to perform (micro) pollutant wastewater treatment modelling studies. Sci. Total Environ. 569–570, 278–290.
Solon, K., Flores-Alsina, X., Kazadi Mbamba, C., Volcke, E.I.P., Tait, S., Batstone, D.J., Gernaey, K.V., Jeppsson, U., 2015. Effects of ionic strength and ion pairing on (plant-wide) modelling of anaerobic digestion processes. Water Res. 70, 235–245.

Stumm, W., Morgan, J.J., 1996. In: Schnoor, J.L., Zehnder, A. (Eds.), Aquatic Chemistry: Chemical Equilibria and Rates in Natural Waters. John Wiley and Sons, New York, NY, USA.
Sweetapple, C., Fu, G., Butler, D., 2014. Multi-objective optimisation of wastewater treatment plant control to reduce greenhouse gas emissions. Water Res. 55, 52–62.
Takács, I., Patry, G.G., Nolasco, D., 1991. A dynamic model of the clarification thickening process. Water Res. 25 (10), 1263–1271.
Tchobanoglous, G., Burton, F.L., Stensel, H.D., 2003. Wastewater Engineering: Treatment and Reuse, fourth ed. Massachusetts, USA: McGraw-Hill Education, Boston.
Truskey, G., Yuan, F., Katz, D.F., 2009. Transport Phenomena in Biological Systems (Upper Saddle River, New Jersey, USA: Prentice Hall).
Vaneeckhaute, C., 2015. Nutrient Recovery from Bio-digestion Waste: from Field Experimentation to Model-based Optimization. Université Laval, Québec, Canada. PhD thesis.
Vaneeckhaute, C., Lebuf, V., Michels, E., Belia, E., Vanrollegem, P.A., Tack, F.M.G., Meers, E., 2017. Nutrient recovery from digestate: systematic technology review and product classification. Waste Biomass Valorizat. 8 (1), 21–40.
van Rensburg, P., Musvoto, E.V., Wentzel, M.C., Ekama, G.A., 2003. Modelling multiple mineral precipitation in anaerobic digester liquor. Water Res. 37 (13), 3087–3097.
Vanrolleghem, P.A., Corominas, L., Flores-Alsina, X., 2010. Real-time control and effluent ammonia violations induced by return liquor overloads. Proc. Water Environ. Fed. 2010 (9), 7101–7108.
Vanrolleghem, P.A., Flores-Alsina, X., Guo, L., Solon, K., Ikumi, D., Batstone, D.J., Brouckaert, C., Takács, I., Grau, P., Ekama, G.A., Jeppsson, U., Gernaey, K.V., 2014. Towards BSM2-GPS-X: a plant-wide benchmark simulation model not only for carbon and nitrogen, but also for greenhouse gases (G), phosphorus (P), sulphur (S) and micropollutants (X), all within the fence of WWTPs/WRRFs. In: Proceedings of the IWA/WEF Wastewater Treatment Modelling Seminar, Spa, Belgium, 30 March-2 April 2014.
Vanrolleghem, P.A., Vaneeckhaute, C., 2014. Resource recovery from wastewater and sludge: modelling and control challenges. In: Proceedings of the IWA Specialist Conference on Global Challenges for Sustainable Wastewater Treatment and Resource Recovery, Kathmandu, Nepal, 26–30 October 2014.
Verstraete, W., Van de Caveye, P., Diamantis, V., 2009. Maximum use of resources present in domestic "used water". Bioresour. Technol. 100 (23), 5537–5545.
Volcke, E.I.P., Gernaey, K.V., Vrecko, D., Jeppsson, U., van Loosdrecht, M.C.M., Vanrolleghem, P.A., 2006a. Plant-wide (BSM2) evaluation of reject water treatment with a SHARON-Anammox process. Water Sci. Technol. 54 (8), 93–100.
Volcke, E.I.P., van Loosdrecht, M.C.M., Vanrolleghem, P.A., 2006b. Continuity-based model interfacing for plant-wide simulation: a general approach. Water Res. 40 (15), 2817–2828.
Wang, R., Yongmei, L., Chen, W., Zou, J., Chen, Y., 2016. Phosphate release involving PAOs activity during anaerobic fermentation of EBPR sludge and the extension of ADM1. Chem. Eng. J. 297 (1), 436–447.
Wentzel, M., Ekama, G., Sotemann, S., 2006. Mass balance based plant wide treatment model – Part 1. Biodegradability of wastewater organics under anaerobic conditions. Water sa. 32 (3), 2675–2692.
Xu, X., Chen, C., Lee, D.J., Wang, A., Guo, W., Zhou, X., Guo, H., Yuan, Y., Ren, N., Chang, J.S., 2013. Sulfate-reduction, sulfide-oxidation and elemental sulfur bioreduction process: modeling and experimental validation. Bioresour. Technol. 147, 202–211.
Zaher, U., Grau, P., Benedetti, L., Ayesa, E., Vanrolleghem, P.A., 2007. Transformers for interfacing anaerobic digestion models to pre- and post-treatment processes in a plant-wide modelling context. Environ. Model. Softw. 22 (1), 40–58.
Zhang, J., Zhang, Y., Chang, J., Quan, X., Li, Q., 2013. Biological sulfate reduction in the acidogenic phase of anaerobic digestion under dissimilatory Fe (III)-reducing conditions. Water Res. 47 (6), 2033–2040.